

Mixed Lubrication of Coupled Journal-Thrust Bearing Systems

Yansong Wang,¹ Q. Jane Wang¹ and Chih Lin²

Abstract: Many mechanisms, such as computer hard drives, gear trains, and machine tool spindle systems, operate under both axial and radial loads, which should be respectively supported by a thrust and a journal bearing. By utilizing the end face of the shaft of a journal bearing as a thrust bearing, a coupled journal-thrust bearing system can be formed. This paper presents a mixed lubrication model developed to investigate the lubrication of this coupled bearing system. A conformal-mapping method is used in the model formulation to facilitate a universal flow description. The performance of typical coupled bearing systems is numerically investigated.

keyword: Mixed lubrication, conformal mapping, coupled bearing system

1 Introduction

Many mechanisms, such as computer hard drives, gear trains, and machine tool spindle systems, operate under combined radial and thrust loads which may be separately supported by a radial and a thrust bearing. However, in many applications, the end face of the shaft in a journal bearing is utilized to form a hydrodynamic thrust bearing, thus creating a coupled journal and thrust bearing. Figure 1(a) presents a schematic of such a bearing system. An angular misalignment between the centerlines of the shaft and the bearing produces a geometric condition conducive for the thrust bearing hydrodynamic effect. The side leakage flow from the journal bearing serves as a natural lubricant supply to the thrust bearing. Arising from improper assembly practices and structural deflection, the angular misalignment determines the orientation of the end face of the shaft and creates two wedges in the thrust bearing: one in the radial direction and the other in the circumferential direction. The wedges are defined with respect to the center-

line of the thrust bearing. Angular misalignment between the shaft and the bearing has been shown to strongly affect the lubrication of the journal bearing (Wang, Zhang, Wang and Lin, 2002). The formation of the wedges will be described in more details in the next section. The thrust bearing so formed is different from the conventional tilting-pad thrust bearing because its lubrication is affected by both the geometric and the hydrodynamic coupling with the journal bearing.

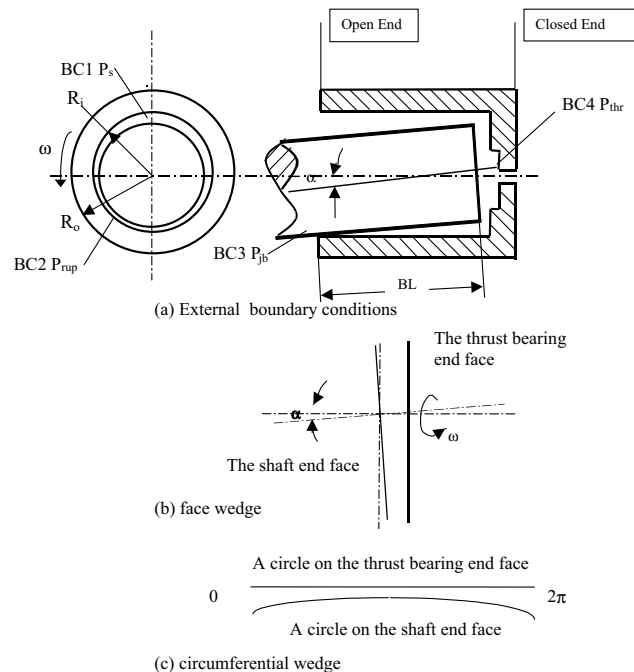


Figure 1 : Schematic of journal bearing and the end thrust bearing formed by shaft misalignment

Information on the modeling of the coupled journal and thrust bearings is very limited. Most of the research effort in this area is concentrated on aerostatic journal-thrust bearings, or the Yates bearings (Tawfik and Stout 1981, Pander 1986), for applications such as the supports for hard disk drives and gas bearings. Usually, the bearing system for hard disk drives consists of small

¹ Department of Mechanical Engineering
Northwestern University, Evanston, IL 60208, U.S.A.

² Baker Hughes, Inc., Houston, TX 77252

journal bearings and small thrust bearings for very light loads (Zhang, 1999). The characteristics of this kind of journal-thrust bearing pair have been studied for full-film hydrodynamic lubrication under perfectly aligned geometric conditions (Tawfik and Stout 1981, Pander and Pandit 1986, Tieu 1991, Zang and Hatch 1995, and Lie and Bhat 1995). Very little comprehensive analysis exists that investigates the performance of the coupled bearing system operating under mixed lubrication conditions.

This paper presents a mixed lubrication model for a coupled journal-thrust bearing with angular misalignment. A conformal-mapping method that facilitates a universal flow description is explored and used in the model formulation.

2 Description of the Coupled Journal-Thrust Bearing System

Figure 1(a) illustrates the geometry of a journal-thrust bearing system that consists of a shaft and a bearing cylinder with one open end. The angular misalignment, α , is defined between the centerlines of the shaft and the bearing which arises from improper shaft assembly practices and structural deflection. The bearing is subject to both radial and thrust loads. There are two wedges formed due to the shaft misalignment. The wedge in the radial direction of the thrust bearing, or the face width direction, as shown in Figure 1(b), is called the “face wedge”. The wedge along the circumferential direction, as shown in Figure 1(c), by the extended perimeters of a pair of circles from the end face of the shaft and the outer edge of the thrust bearing, is called the “circumferential wedge”. The wedge is said to be convergent if the flow is from the larger clearance side to the smaller clearance side.

In the mathematical development of the model for the coupled bearing described above, the lubricant is assumed to be an incompressible fluid with a constant density. Lubricant flows are treated as steady-state laminar flows. Moreover, the hydrodynamic pressure is considered to be constant through the film thickness.

2.1 Governing equations

The average Reynolds equation derived by Patir and Cheng (1978) is employed to describe the pressure-film thickness relation for the thrust bearing in mixed lubrication. The average Reynolds equation in the cylindrical

coordinate has the following form:

$$\frac{\partial}{\partial r}(\phi_r \frac{h^3 r}{\mu} \frac{\partial p}{\partial r}) + \frac{1}{r} \frac{\partial}{\partial \theta}(\phi_\theta \frac{h^3}{\mu} \frac{\partial p}{\partial \theta}) = 6\omega r (\frac{\partial h_T}{\partial \theta} - \sigma \frac{\partial \phi_s}{\partial \theta}) \quad (1)$$

where ϕ_r and ϕ_θ are the pressure flow factors and ϕ_s is the shear flow factor defined by Patir and Cheng. The film thickness is described by the following formula:

$$h(r, \theta) = h_0 + r \tan \alpha \cos \theta \quad (2)$$

In this equation, h_0 is the average film thickness of the thrust bearing measured at its center and α is the misalignment angle. Coordinates, (r, θ) , define a point on the end face of the shaft, as shown in Figure 2. The governing equation for the journal bearing is expressed in the Cartesian coordinate system where $x = R_j \theta$.

$$\begin{aligned} \frac{\partial}{\partial x}(\phi_x \frac{h^3}{12\mu} \frac{\partial p}{\partial x}) + \frac{\partial}{\partial z}(\phi_z \frac{h^3}{12\mu} \frac{\partial p}{\partial z}) \\ = \frac{U_1 + U_2}{2} \frac{\partial h_T}{\partial x} + \frac{U_1 - U_2}{2} \sigma \frac{\partial \phi_s}{\partial x} \end{aligned} \quad (3)$$

The film thickness of the journal bearing is expressed by:

$$h(\theta, z) = c(1 + \varepsilon \cos(\theta - \phi)) + \alpha(z - BL/2) \cos(\theta - \phi) \quad (4)$$

where, ε , the eccentricity ratio, is the ratio of e , the distance between the centers of the journal and the bearing, over the bearing radial clearance c .

Asperity interaction is one of the main features of mixed lubrication. Since the film thickness varies circumferentially, a relationship between the asperity contact pressure and the film thickness in terms of the average gap is needed in order to compute the asperity contact load. The rough-surface contact model by Lee and Ren (1996) was employed in this study.

2.2 Boundary conditions

Four external pressure boundaries involved in this coupled bearing system, as shown in Figure 1(a), are listed here:

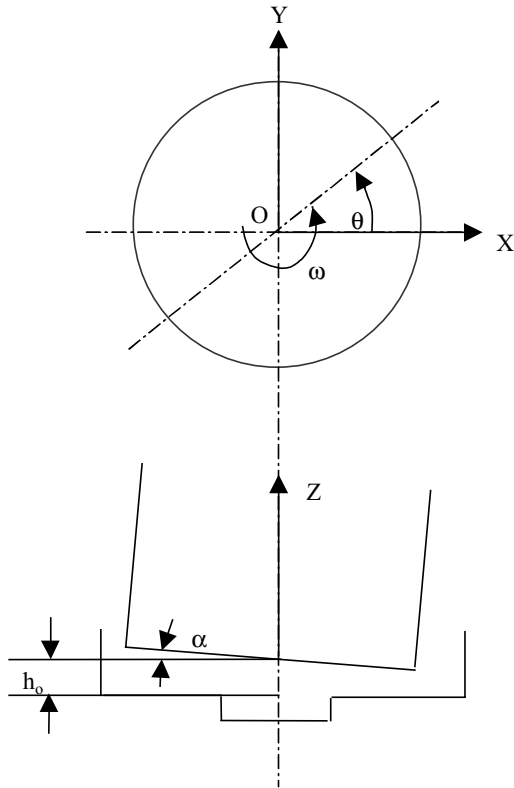


Figure 2 : Film thickness calculation for the thrust bearing

BC1, the pressure of journal-bearing lubricant supply, p_s ,

BC2, the film rupture pressure, p_{rup} ,

BC3, the journal-bearing environment pressure, p_{jb} , at the journal bearing side, and

BC4, the thrust-bearing environment pressure, p_{thr} , at the inner edge of the annular end face of the bearing that forms the thrust bearing.

In the cavitation region, Reynolds boundary conditions are used for both journal and thrust bearings. There is also an internal boundary along the interface between the journal bearing and the thrust bearing where the continuity of flow rates and pressures must be satisfied. Each bearing has two flows: the circumferential flow and the side flow for the journal bearing and the circumferential flow and the radial flow for the thrust bearing. The side flow in the journal-bearing is connected to the radial flow of the thrust bearing. The flow rates over the coupling interface may be expressed by the average flows

$$\begin{aligned}\bar{q}_\theta &= \phi_\theta \frac{h^3}{12\mu r} \frac{\partial p}{\partial \theta} + \frac{U}{2}h + \frac{U}{2}\sigma\phi_s \\ \bar{q}_r &= \phi_r \frac{h^3}{12\mu} \frac{\partial p}{\partial r}\end{aligned}\quad (5)$$

Because the flow rate continuity in the circumferential direction is automatically satisfied, only the continuity in the radial direction of the thrust bearing and the width direction of the journal bearing needs to be treated. The flow rate continuity condition may be expressed as

$$\frac{h_j^3}{12\mu} \frac{p_0 - p_t}{\Delta r} = \frac{h_{thr}^3}{12\mu} \frac{p_j - p_0}{\Delta z}\quad (6)$$

The internal pressure, p_0 , along the interface of thrust and journal bearing can be solved from Equation (6) and expressed as

$$p_0 = \frac{\frac{h_j^3}{\Delta r} p_t + \frac{h_{thr}^3}{\Delta z} p_j}{\frac{h_j^3}{\Delta r} + \frac{h_{thr}^3}{\Delta z}}\quad (7)$$

2.3 Load balance

The load applied to the bearing system is illustrated in Figure 3. Both force equilibrium and moment balance given in Equations (8) and (9) must be satisfied.

$$\begin{aligned}\text{X direction: } W_T - W_{Ta} - W_{Tf} &= 0 \\ \text{Z direction: } W_J - W_{Ja} - W_{Jf} &= 0\end{aligned}\quad (8)$$

$$W_J L_J + W_{Tf} L_{Tf} + W_{Ta} L_{Ta} - W_{Ja} L_{Ja} - W_{Jf} L_{Jf} = 0\quad (9)$$

Where

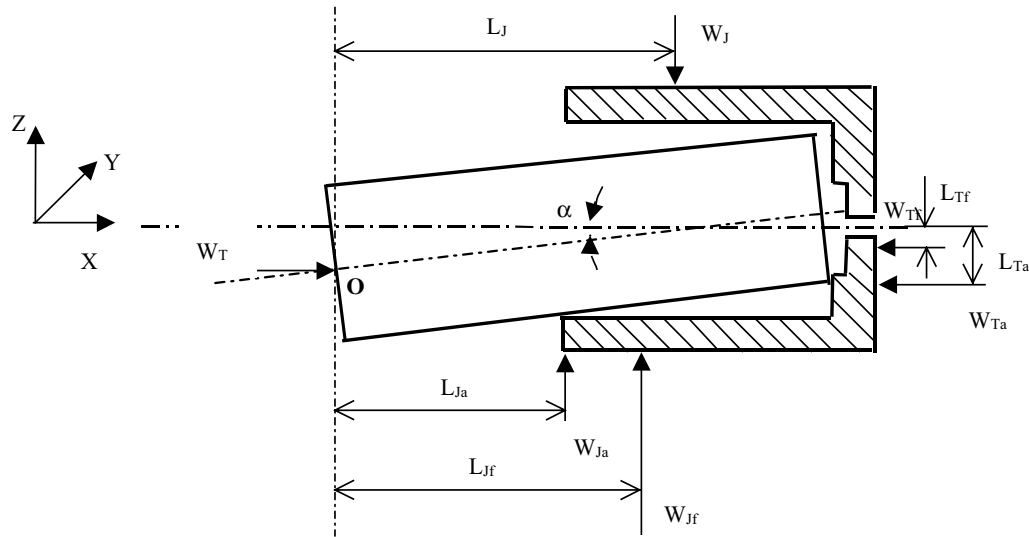


Figure 3 : Schematic of the load balance in the coupled journal-thrust bearing system

$$W_{Tf} = \int_0^R p_{Tf} 2\pi r dr$$

$$W_{Ta} = \int_0^R p_{Ta} 2\pi r dr$$

$$W_{Jf} = \iint p_{Jf} \cos \phi R d\phi dz$$

$$W_{Ja} = \iint p_{Ja} \sin \phi R d\phi dz$$

2.4 Conformal mapping and a universal equation

A conformal mapping method (Nehari 1975) is utilized to transform the end face of the thrust bearing from its annular (physical) domain to a rectangular (computational) domain formed by the extended geometry of the journal bearing. An exponential function and a logarithmic function given in Table 1 form a pair of mapping that facilitate such domain conversion. By employing the logarithmic function, the end face of the thrust bearing can be mapped into a rectangular shape whose edges conform well with the geometry of the extended journal surface. The correspondence between the mapped domain and the physical domain is shown in Figure 4(a). With the introduction of this conformal mapping, the problem for the coupled journal-thrust bearing can be simplified from a 3-D space domain into a 2-D plane domain. By using the transformation function, $x = \ln(r/R_1)$, and $y = \theta$, a physical point, (r, θ) , on the thrust bearing end face is mapped into a point, (x, y) , in the computational domain.

In the mapping, r has two expressions, $r = R_1$ for $x = 0$, and $r = R_2$ for $x = \ln(R_2/R_1)$. Using the chain rule of differentiation, $\frac{\partial}{\partial r} = \frac{\partial}{\partial x} \frac{\partial x}{\partial r}$ and $\frac{\partial}{\partial \theta} = \frac{\partial}{\partial y} \frac{\partial y}{\partial \theta}$, and the inverse Jacobian matrix, $J^{-1} = \det \begin{pmatrix} \frac{\partial r}{\partial x} & \frac{\partial \theta}{\partial x} \\ \frac{\partial r}{\partial y} & \frac{\partial \theta}{\partial y} \end{pmatrix}$, the governing equation for the thrust bearing takes the following form:

$$\frac{\partial}{\partial x} \left(\phi_x \frac{h^3}{\mu} \frac{\partial p}{\partial x} \right) + \frac{\partial}{\partial y} \left(\phi_y \frac{h^3}{\mu} \frac{\partial p}{\partial y} \right) = 6\omega R_1^2 e^{2x} \left(\frac{\partial h_T}{\partial y} + \sigma \frac{\partial \phi_s}{\partial y} \right) \tag{10}$$

where $0 \leq x \leq \ln(R_2/R_1)$ and $0 < y \leq 2\pi$.

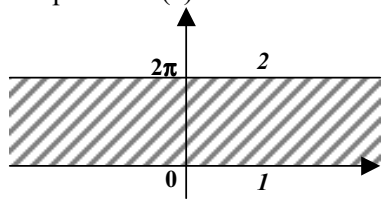
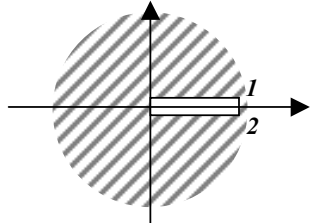
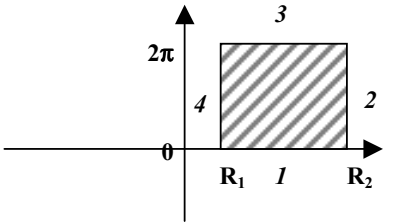
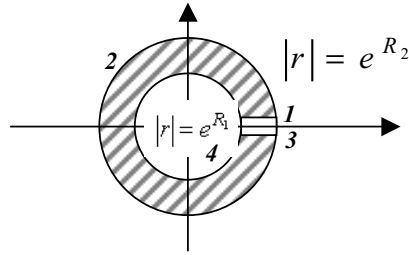
The governing equation for the journal bearing becomes

$$R_2^2 \frac{\partial}{\partial x} \left(\phi_x \frac{h^3}{\mu} \frac{\partial p}{\partial x} \right) + \frac{\partial}{\partial y} \left(\phi_y \frac{h^3}{\mu} \frac{\partial p}{\partial y} \right) = 6\omega R_2^2 \left(\frac{\partial h_T}{\partial y} + \sigma \frac{\partial \phi_s}{\partial y} \right) \tag{11}$$

where $x : (-BL, 0)$ and $y : (0, 2\pi)$.

A universal equation can be obtained by combining the governing equations for the journal bearing and the thrust bearing

Table 1 : Exponential conformal mapping pairs

z-plane	r-plane
<p>Infinite strip $0 < \text{Im}(z) \leq 2\pi$</p> 	<p>Plane, cut along positive real axis</p> 
	

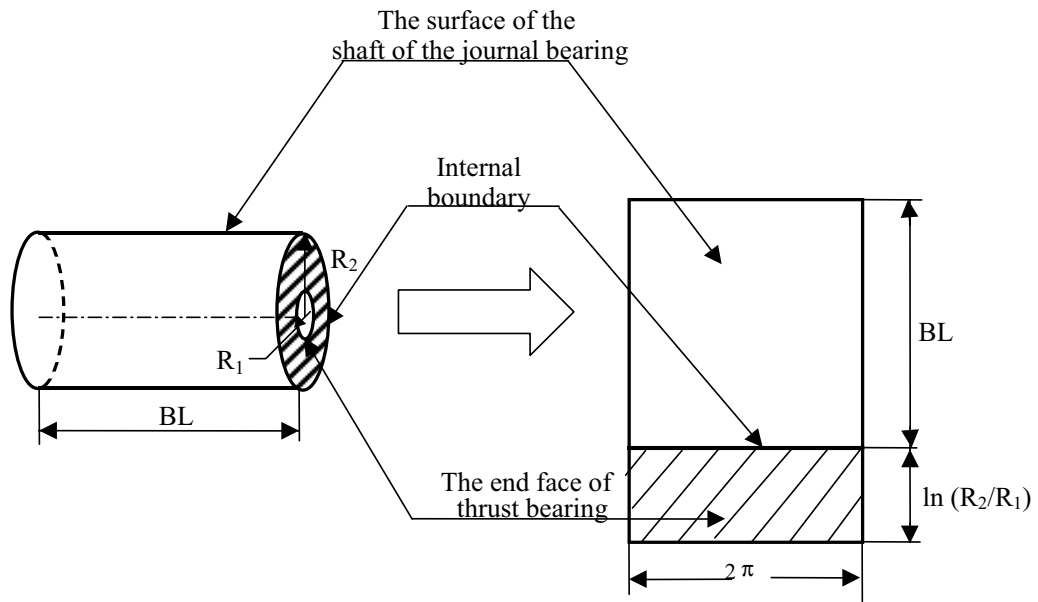


Figure 4 : Conformal mapping the transfers the thrust bearing surface into a rectangular computational domain which is connected to the journal bearing domain

$$G_1 \frac{\partial}{\partial x} \left(\phi_x \frac{h^3 \partial p}{\mu \partial x} \right) + \frac{\partial}{\partial y} \left(\phi_y \frac{h^3 \partial p}{\mu \partial y} \right) = 6\omega G_2 \left(\frac{\partial h_T}{\partial y} + \sigma \frac{\partial \phi_s}{\partial y} \right) \quad (12)$$

where

$$G_1 = 1, G_2 = R_1^2 e^{2x} \\ \text{for the thrust bearing } (x \geq 0)$$

$$G_1 = R_2^2, G_2 = R_2^2 \\ \text{for the journal bearing } (x < 0)$$

Equation (11) includes the internal boundary as a part of the computational domain. Thus the conditions for pressure and flow rate continuity are satisfied automatically. If the mapping method were not used, one would have to sweep the computation from thrust bearing domain to journal bearing domain, or vice versa. The flow-rate and pressure continuity conditions along the coupling interface would have to be explicitly utilized, and different governing equations have to be applied. The mapping method introduced in this work greatly simplifies the solution process, and the entire bearing system can be solved simultaneously without handling any internal boundary condition. It also significantly reduces the CPU time. Table 2 compares the computation time (on a PII450 computer) and the results obtained from the mapping method and direct sweeping method, where the journal-thrust bearing has a positive misalignment angle 0.05° , the thrust bearing average film thickness is $60\mu\text{m}$ and the journal bearing eccentricity ratio is 0.8. The results are in good agreement, however the mapping method saves 40% of the computation time.

The solution accuracy is controlled as $\frac{\max |p_0^{(n+1)} - p_0^{(n)}|}{\max |p_0^{(n)}|} < 0.004$. The current model formulation has been verified by solving separately a journal bearing problem and a thrust bearing problem.

3 Possible Forms of the Journal-Thrust Bearing Coupling

In this section, we consider three possible forms of journal-thrust bearing coupling:

(a) Coupled bearings with positive misalignment angles. The misalignment angle is defined as positive if the centerline of the shaft is rotated counter-clockwise by an

Table 2 : Performance comparison between mapping method and direct sweeping method

	Mapping method	Direct sweeping method
Thrust bearing pressure peak (MPa)	3.69	3.67
Journal bearing pressure peak (MPa)	4.91	4.88
Computation time (minutes)	12	20

angle α , as shown in Figure 5(a). The pressurized region in the journal bearing develops along the lower side (pressure side) of the shaft, but the peak pressure occurs towards the open end of the journal bearing where the clearance is the minimum. The thrust bearing so configured forms a divergent face wedge towards the centerline of the thrust bearing and a convergent circumferential wedge with respect to the flow direction at the pressure side of the bearing system.

(b) Coupled bearings with negative misalignment angles. Referring to Figure 1(a), a negative misalignment angle is defined as the centerline of the journal bearing rotating clockwise about an axis pointing out of the paper. Figure 5(b) shows the bearing system with a negative misalignment angle. In this case, the peak hydrodynamic pressure in the journal bearing occurs near the closed end of the pressure side of the journal bearing. The thrust bearing so configured forms a convergent face wedge towards the centerline of the thrust bearing in a region corresponding to the pressure side of the journal bearing. The circumferential wedge converges at the location about 180° from pressure side of the journal bearing.

(c) Hydrodynamically decoupled journal and thrust bearings. It is possible that the journal bearing and the thrust bearing act independently as far as their hydrodynamics is concerned. One such case is when the radius of the fillet at the interface of the coupled bearing is sufficiently large as if there were several lubricant exit holes, such as those shown in Figure 5(c). Under this circumstance, the journal bearing and the thrust bearing may operate independently without any hydrodynamic coupling effect even though they are still geometrically coupled. The

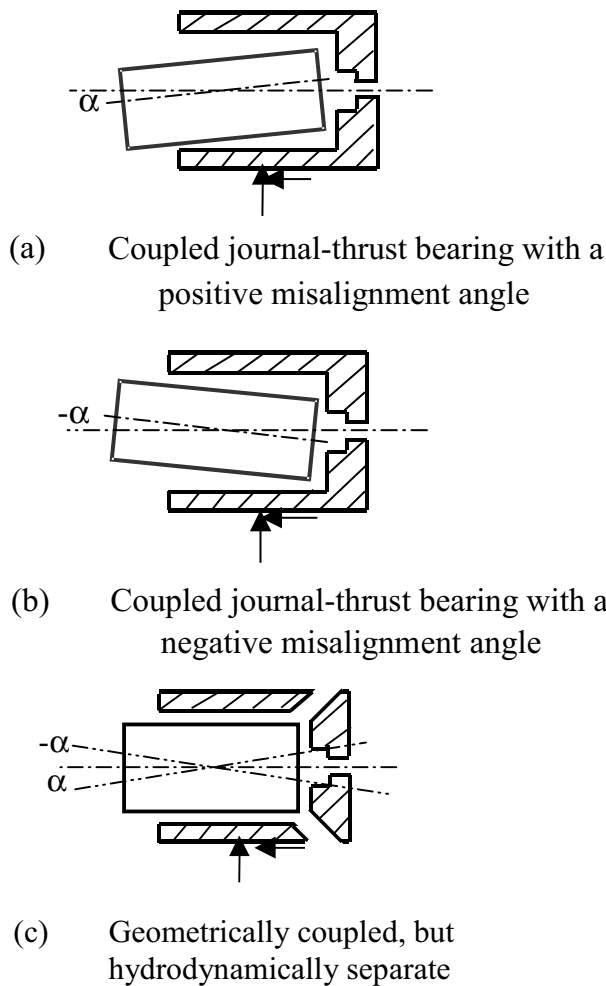


Figure 5 : Configurations of the coupled journal-thrust bearing

sign of the misalignment angle determines the geometric coupling effect, as described in Figures 5(a) and 5(b). For this case, the governing equations for the journal and thrust bearings have to be solved separately.

4 Results and Discussion

Typical coupled journal-thrust bearing systems with the coupling arrangement mentioned above are numerically investigated. Referring to Figure 1, the outer radius (R_o), inner radius (R_i), and the bearing length (BL) of the bearing sleeve are 46.35 mm, 40.00 mm, and 31.11 mm, respectively. The inner radius of the thrust bearing is 10.00 mm and the outer radius is the same as the outer radius of the journal shaft (Fig. 4). The journal bearing radial clearance is 0.152 mm. The bearing rotational speed con-

sidered in this study is 1000 revolution per minute. The journal bearing eccentricity ratio, the misalignment angle and the thrust bearing average film thickness are three independent parameters that are specified for each case analyzed. Figures 6 through 10 show the results of the analysis, where pressure distributions are plotted in the computational domain: the radial hydrodynamic pressure distribution in the journal-bearing region and the thrust hydrodynamic pressure distribution in the thrust-bearing region. The integration of the pressure in the journal-bearing region yields the radial load and that of the pressure in the thrust-bearing region gives the thrust load.

The performance of the journal-thrust bearing system with a positive misalignment, $\alpha = 0.05^\circ$, at two different journal bearing eccentricity ratios, 0.8 and 0.9 is presented in Figures 6 and 7. The average thrust bearing film thickness is $60 \mu\text{m}$ for the case shown in Figure 6 and is $40 \mu\text{m}$ for the case shown in Figure 7. Figures 6(a), 6(c), 7(a) and 7(c) are for the cases of a coupled journal-thrust bearing system with the positive misalignment angle of 0.05° . Figures 6(b), 6(d), 7(b) and 7(d) are for cases of a hydrodynamically decoupled bearing with the same positive misalignment angle. As expected, in the cases of positive misalignment angles the hydrodynamic pressure in the journal bearing rises towards the open end of the journal bearing where the film thickness is the minimum. The hydrodynamic pressure in the thrust bearing is generated by the convergent circumferential wedge in the region corresponding to the pressure side of the journal bearing and is further boosted by the pressurized flow from the journal bearing if hydrodynamic coupling exists. The divergent face wedge in this case has little contribution to the hydrodynamic pressure generation. For an eccentricity ratio of 0.8, the hydrodynamic coupling raises the maximum hydrodynamic pressure in the thrust bearing nearly five times higher than that in the hydrodynamically decoupled case when comparing Figure 6(a) with Figure 6(b). In addition, the maximum hydrodynamic pressure in the journal bearing is raised by about 42%, which arises naturally as the leakage is inhibited by the hydrodynamically coupled thrust bearing.

By referring to Figures 6(c) and 6(d), increasing the journal bearing eccentricity ratio from 0.8 to 0.9 dramatically increases the hydrodynamic pressure in the journal bearing, typically, by more than eight-fold with both hydrodynamically coupled or decoupled bearings in the case studies. Correspondingly, the maximum hydrodynamic

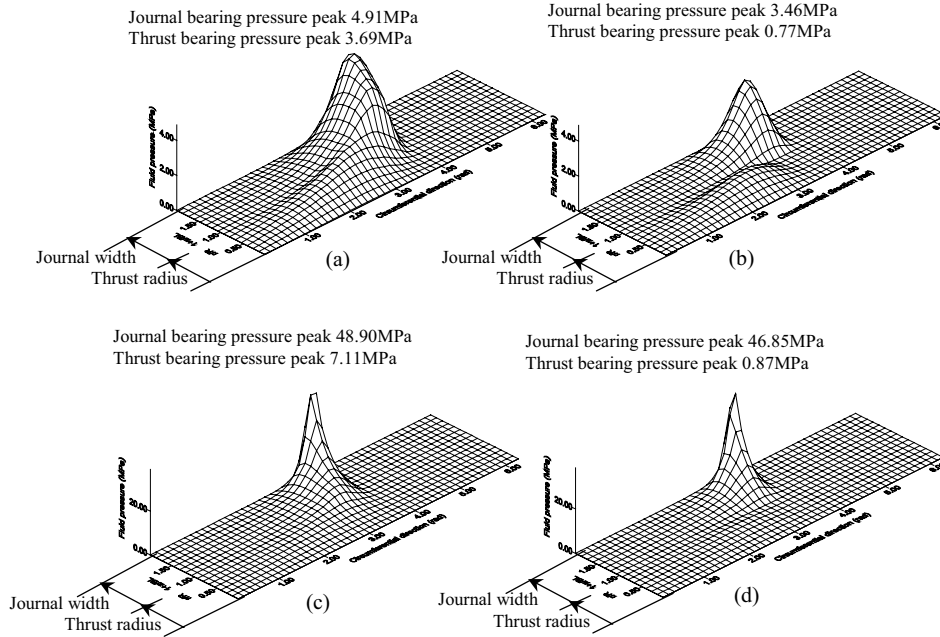


Figure 6 : Coupling effect on the performance of the journal-thrust bearing with a positive misalignment angle $\alpha = 0.05^\circ$ and a larger thrust bearing average film thickness $h_0 = 60\mu\text{m}$. (a) $\epsilon = 0.8$ with the hydrodynamic coupling (b) $\epsilon = 0.8$ without the hydrodynamic coupling (c) $\epsilon = 0.9$ with the hydrodynamic coupling (d) $\epsilon = 0.9$ without the hydrodynamic coupling

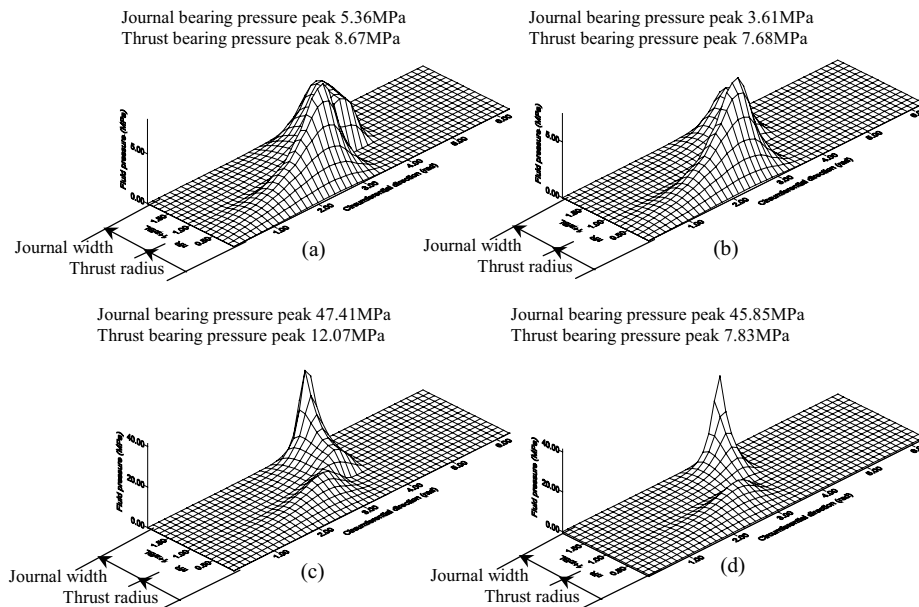


Figure 7 : Coupling effect on the performance of the journal-thrust bearing with a positive misalignment angle $\alpha = 0.05^\circ$ and a smaller thrust bearing average film thickness $h_0 = 40\mu\text{m}$. (a) $\epsilon = 0.8$ with the hydrodynamic coupling (b) $\epsilon = 0.8$ without the hydrodynamic coupling (c) $\epsilon = 0.9$ with the hydrodynamic coupling (d) $\epsilon = 0.9$ without the hydrodynamic coupling

pressure in the thrust bearing rises about 90% higher with the hydrodynamic coupling and is only slightly higher (i.e. 13%) in the case without the coupling.

The hydrodynamic pressure in the thrust bearing further increases if the average film thickness of the thrust bearing is reduced from $60\ \mu\text{m}$ to $40\ \mu\text{m}$ while maintaining the same misalignment angle. Its peak value is higher than that of the journal bearing, whether in the hydrodynamically coupled or decoupled case, when the eccentricity ratio of the journal bearing is at 0.8. The maximum hydrodynamic pressure in the thrust bearing becomes even higher if the journal bearing eccentricity ratio is simultaneously increased to 0.9. However, the increase in the eccentricity ratio mainly favors the journal bearing. As a result, the hydrodynamic pressure in the journal bearing far exceeds that of the thrust bearing and becomes dominant as seen in Figures 7(c) and 7(d).

As indicated previously, increasing eccentricity ratio primarily raises the hydrodynamic pressure in the journal bearing. At a larger eccentricity ratio of 0.9, the pressure distributions in the journal bearing are almost the same whether the hydrodynamic coupling exists or not, as if it were an independent bearing. The reduction of the average film thickness of the thrust bearing has little influence on the journal bearing pressure distribution although the displacement of the shaft increases the actual journal bearing width by $20\ \mu\text{m}$. Nevertheless, the increase of the journal-bearing eccentricity ratio increases the hydrodynamic pressure in the thrust bearing because the pressurized region of the convergent circumferential wedge of the thrust bearing is slightly enlarged.

The hydrodynamic coupling effect imposed by the negative misalignment angle is different from that by the positive misalignment angle as in the former case, the hydrodynamic pressure in both the journal and thrust bearings rises towards the coupling boundary. The minimum film thickness, and thus the maximum hydrodynamic pressure in the journal bearing, takes place close to the coupling boundary, and the side flow from the journal bearing is fed into the convergent face wedge of the thrust bearing, as illustrated in Figure 5(b). Hydrodynamic pressure generation in the thrust bearing comes from a convergent circumferential wedge formed in a region corresponding to the non-pressure side of the journal bearing.

The performance of the bearing system with the negative misalignment angle is shown in Figures 8 and 9. Two pressure peaks appear in the thrust bearing (Fig.

8(a)). The first peak corresponds to the location of the maximum hydrodynamic pressure in the journal bearing where the coupling to the convergent face wedge in the thrust bearing occurs. The second peak occurs at the convergent circumferential wedge. When the two bearings are hydrodynamically coupled and worked under a smaller eccentricity ratio of 0.8, the magnitude of the first peak is greater than that of the second, suggesting that the effect of the face wedge in this case is more prominent than the circumferential wedge. If the bearings are hydrodynamically decoupled, only the second peak mentioned above with a much lower value is present (Fig. 8(b)). Increasing the journal bearing eccentricity ratio to 0.9 raises the hydrodynamic pressures in both the journal and thrust bearings. However, rise in the magnitude of thrust bearing pressure peak, from 1.38 MPa in Figure 8(a) to 1.46 MPa in Figure 8(c), is much lower than that in the positive misalignment angle case, from 3.69 MPa in Figure 7(a) to 7.11 MPa in Figure 7(c).

Decreasing the average film thickness of the thrust bearing from $60\ \mu\text{m}$ to $40\ \mu\text{m}$ further increases the magnitude of the second hydrodynamic pressure peak in the thrust bearing (Fig. 9). Although the magnitude of both of the journal and thrust hydrodynamic pressure increases, the hydrodynamic pressure distribution in the thrust bearing becomes further separated from that in the journal bearing in this case than in the case with a positive misalignment angle (c.f. Fig. 7). The phenomenon may be attributable to the fact that the minimum clearance in the journal bearing due to the negative misalignment and that in the thrust bearings are geometrically 180° apart. Consequently, the lubricant flow, driven by the pressure gradient in the journal bearing into the largest thrust bearing clearance region, has less reinforcement effect. The contribution to hydrodynamic pressure generation from the circumferential wedge is observed to be more substantial than that from the face wedge when the average film thickness in the thrust bearing is small.

The load carrying capacity of the coupled journal-thrust bearing is of great interest to bearing designers. In Figures 10(a) and 10(b), the performance of the coupled bearing in terms of the load carrying capacity is plotted as a function of the average thrust bearing film thickness, h_0 , for both of the positive and negative misalignment angles at an eccentricity ratio of 0.8. As shown, the load carrying capacity is not sensitive to the sign of the misalignment when the bearing is not hydrodynam-

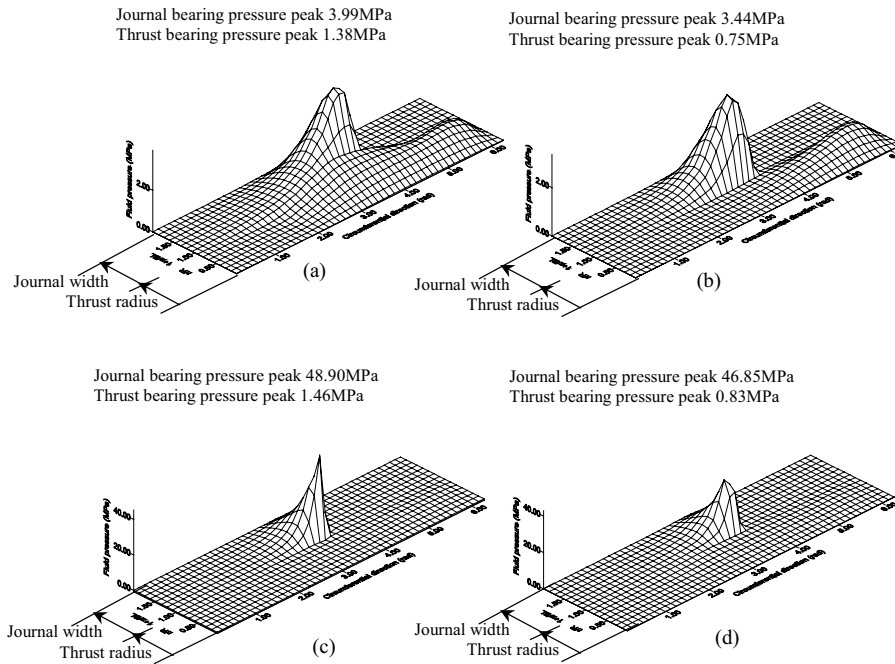


Figure 8 : Coupling effect on the performance of the journal-thrust bearing with a negative misalignment angle $\alpha = -0.05^\circ$ and a larger thrust bearing average film thickness $h_0 = 60\mu\text{m}$. (a) $\epsilon = 0.8$ with the hydrodynamic coupling (b) $\epsilon = 0.8$ without the hydrodynamic coupling (c) $\epsilon = 0.9$ with the hydrodynamic coupling (d) $\epsilon = 0.9$ without the hydrodynamic coupling

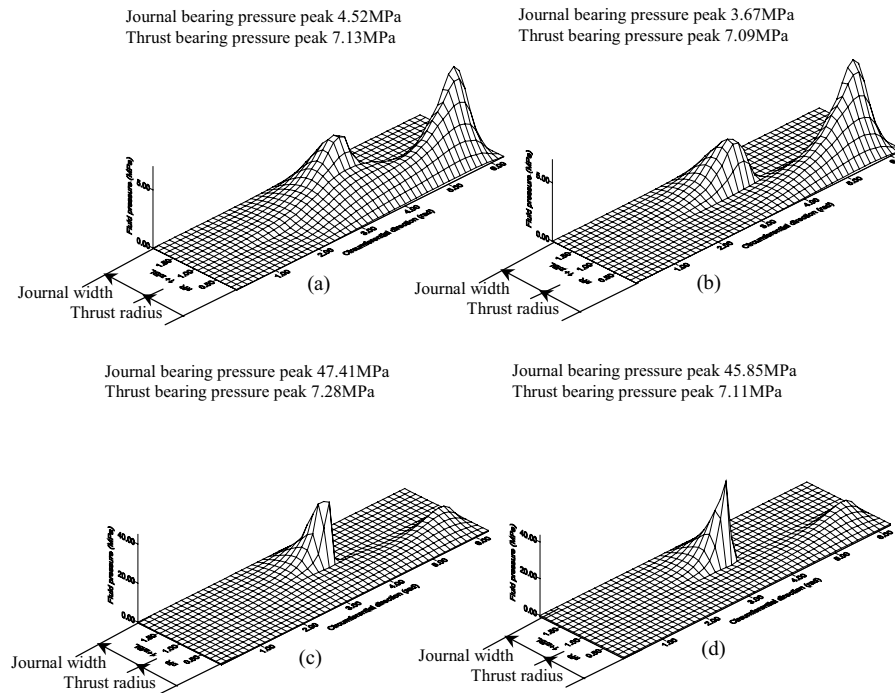
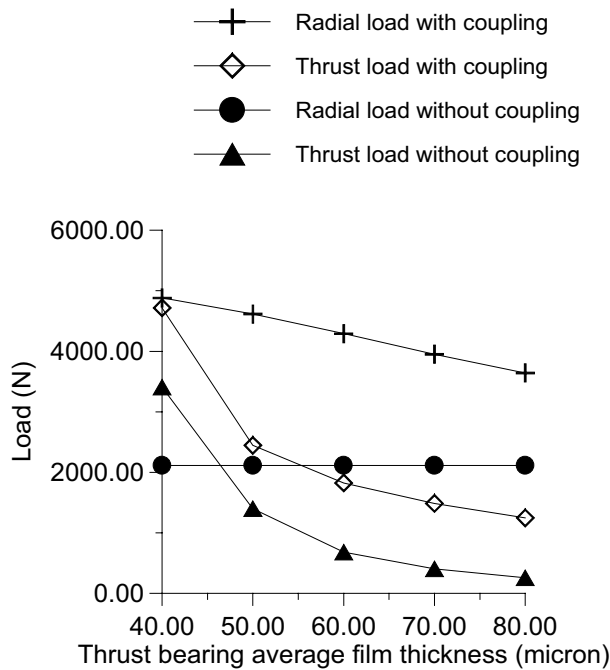


Figure 9 : Coupling effect on the performance of the journal-thrust bearing with a negative misalignment angle $\alpha = -0.05^\circ$ and a smaller thrust bearing average film thickness $h_0 = 40\mu\text{m}$. (a) $\epsilon = 0.8$ with the hydrodynamic coupling (b) $\epsilon = 0.8$ without the hydrodynamic coupling (c) $\epsilon = 0.9$ with the hydrodynamic coupling (d) $\epsilon = 0.9$ without the hydrodynamic coupling



(a)

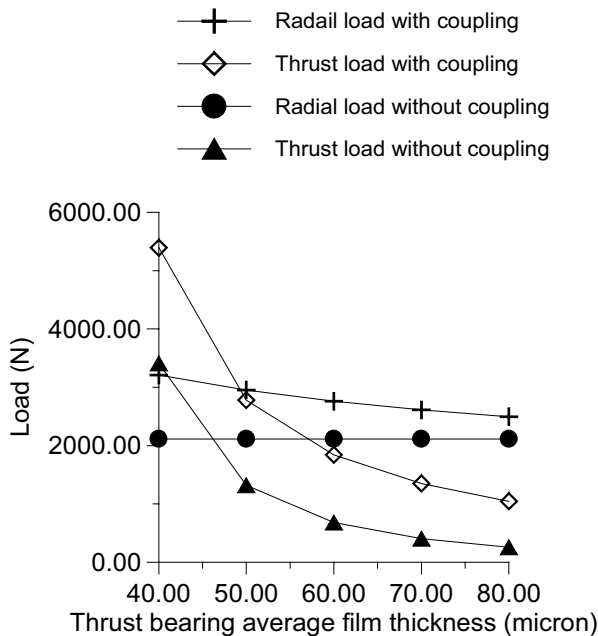
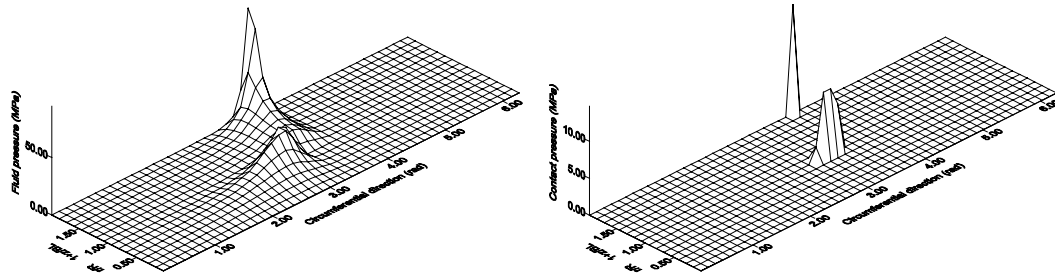


Figure 10 : Load carrying capacity as a function of the average thrust-bearing film thickness, h_0 . (a) $\alpha = 0.05^\circ$, $\epsilon = 0.8$ (b) $\alpha = -0.05^\circ$, $\epsilon = 0.8$

ically coupled. Hydrodynamic coupling improves the load carrying capacity of both the journal and thrust bearings with either misalignment arrangement. A positive misalignment angle increases both the radial and thrust load carrying capacity of the bearing, while a negative misalignment angle primarily enhances the thrust bearing performance. In addition, load carrying capacity of the thrust bearing at a small average film thickness in the case with a negative misalignment angle is greater than that with a positive misalignment angle. It may be attributable to the reinforcement effect between the face and circumferential wedges both being active.

In Figure 11, a case is presented to show the effects with the occurrence of asperity contacts, in which the journal eccentricity ratio is increased to 0.91 and the average film thickness in the thrust bearing is reduced to $35\mu\text{m}$. Figures 11(a) and 11(b) are the results for a bearing system that has a positive misalignment angle of 0.05° with and without the hydrodynamic coupling, respectively. Figure 11(c) is for a hydrodynamically coupled bearing system with a negative misalignment angle of -0.05° . Asperity contact occurs in both the journal and thrust bearings in the area corresponding to the minimum film thickness. For the case of $\alpha = 0.05^\circ$, the contact regions are located at the open end (lower left) of the journal bearing and on the thrust bearing face corresponding to the pressure side of the journal bearing. For the case of $\alpha = -0.05^\circ$, it is located at the closed end of the journal bearing (lower right) and on the thrust bearing face corresponding to the non-pressure side of the journal bearing.

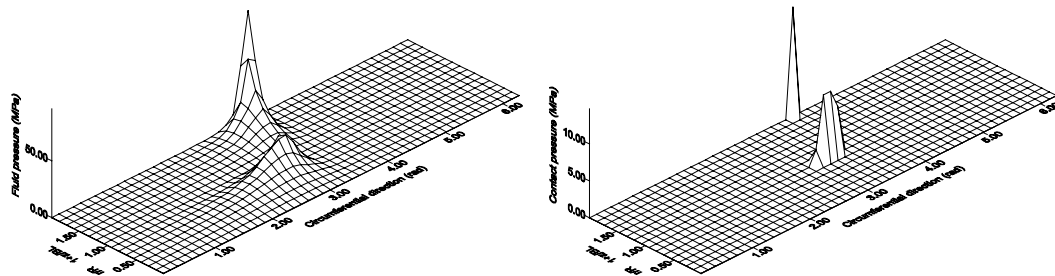
The coupled bearing system in mixed lubrication in three different geometric configurations is shown in Table 3. The results show that, for the same eccentricity ratio and average thrust bearing film thickness, the journal angular misalignment, whether positive or negative, promotes hydrodynamic pressure generation in the thrust bearing. It also demonstrated that through hydrodynamic coupling, the load carrying capacity of both journal and thrust bearings can be increased significantly, especially if a positive misalignment angle is maintained. The radial load capacity can potentially be more than doubled and the thrust load capacity, tripled. In the case of a negative misalignment at such large eccentricity ratio, the minimum film thickness in the journal bearing near the coupling boundary is much smaller than that for the cases shown in Fig. 10, limiting the lubricant flow to the thrust bearing, resulting in a less effective hydrodynamic pres-



Hydrodynamic pressure distribution

Contact pressure distribution

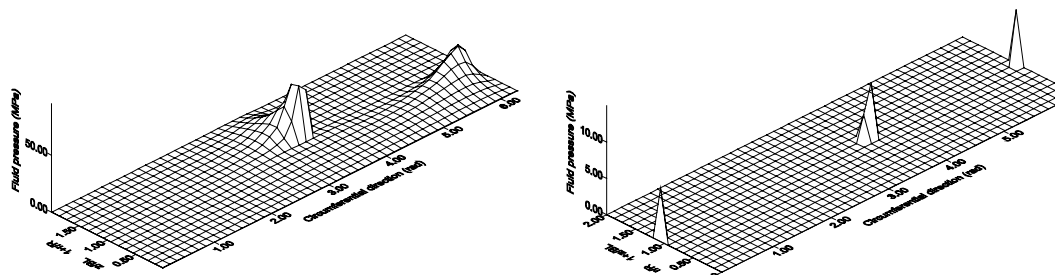
(a)



Hydrodynamic pressure distribution

Contact pressure distribution

(b)



Hydrodynamic pressure distribution

Contact pressure distribution

(c)

Figure 11 : Performance of the coupled journal-thrust bearing with asperity contact ($\epsilon = 0.91, h_0 = 35\mu\text{m}$). (a) With a misalignment angle $\alpha = 0.05^\circ$ and with the hydrodynamic coupling (b) With a misalignment angle $\alpha = 0.05^\circ$ and without the hydrodynamic coupling (c) With a misalignment angle $\alpha = -0.05^\circ$ and with the hydrodynamic coupling

Table 3 : Comparison of load carrying capacity, $\varepsilon = 0.91$, $h_0 = 35\mu\text{m}$

Misalignment	hydrodynamic coupling	Total Radial load (N)	Total Thrust load (N)
No	No	7384	0
No	Yes	9764	2963
Positive	No	14214	10754
Positive	Yes	20234	11944
Negative	No	13800	10450
Negative	Yes	15630	10630

sure generation in the thrust bearing and therefore lower load carrying capacity.

5 Conclusion

A mixed lubrication model is developed to investigate the lubrication of coupled journal-thrust bearing systems. A conformal mapping method is implemented in the model formulation to facilitate a universal flow description. It was demonstrated that the developed computer code can be used to study hydrodynamic lubrication as well as mixed lubrication, either with or without hydrodynamic coupling, of coupled journal-thrust bearing systems. Cases with two different geometric coupling arrangements as specified by a positive and a negative misalignment angle, respectively, with and without hydrodynamic coupling, are numerically analyzed. Based on the numerical results, the following conclusions can be drawn:

1. In the cases where the journal and thrust bearings are hydrodynamically coupled and have a positive misalignment angle, there exists a reinforcement effect on the hydrodynamic pressure generation in the journal bearing and the thrust bearing. This reinforcement is less effective when the misalignment angle becomes negative.
2. For the cases with a positive misalignment angle, a divergent face wedge towards the centerline of the thrust bearing and a convergent circumferential wedge are formed in the thrust bearing in area corresponding to the pressure side of the journal bearing. Only the circumferential wedge contributes to the generation of the hydrodynamic pressure.
3. For the cases with a negative misalignment angle, both face and circumferential wedges contribute to the hydrodynamic pressure generation and two hydrodynamic pressure peaks occur. However, in this

particular bearing configuration at large eccentricity ratios the minimum film thickness in the journal bearing near the coupling boundary limits the lubricant flow to the thrust bearing, resulting in a less effective hydrodynamic pressure generation in the thrust bearing.

4. The eccentricity ratio in the journal bearing has a strong influence on the hydrodynamic pressure generation in the thrust bearing for the cases with a positive misalignment angle. It has virtually no effect on the hydrodynamics of the cases with a negative misalignment angle.
5. The average film thickness of the thrust bearing has only a minor influence on the distribution of the hydrodynamic pressure in the journal bearing. It, however, can change the relative load carrying capacity of the journal and the thrust bearings.

Acknowledgement: The authors would like to express the sincere gratitude to Baker Hughes, Inc. for the financial support and permission to publish the paper. The authors would also like to thank Mr. Eric Sullivan of Baker Hughes for many valuable suggestions during the course of writing this paper. Y. Wang and Q. Wang would also like to thank the US National Science Foundation for support through Grant CMS-9896291 and US Navy.

Nomenclature

- BL Bearing width
 G Universal equation coefficient
 h Compliance, m
 h_T Average gap, m
 L Distance
 p Pressure, Pa

q Flow rate, m^2/s
 R Radius, m
 U Journal speed, m/s
 $r(x), z$ Radial and width coordinates, m
 W Load, N

Greek letters

α Misalignment angle
 ε Journal bearing eccentricity ratio
 ϕ Flow factor
 φ Bearing angle, radians
 μ Viscosity, PaS
 θ Circumferential coordinate, radians
 ρ Density, kg/m^3
 σ Roughness, μm
 ω Angular velocity, 1/s

Subscripts

o Internal boundary
 $1, 2$ Due to inner thrust, journal radius
 c Contact
 i Due to journal bearing inner radius
 j, J, Jb Journal Bearing
 Ja Due to journal bearing asperity contact pressure
 Jf Due to journal bearing hydrodynamic pressure
 O Due to journal bearing outer radius
 r, θ, z Radial, circumferential, and width directions
 rup Rupture
 s Oil supply, shear flow
 T, thr Thrust bearing
 Ta Due to thrust bearing asperity contact pressure
 Tf Due to thrust bearing hydrodynamic pressure

Reference

- Lee, S. C.; Ren, N.** (1996): Behavior of elastic-plastic rough surface contacts as affected by the surface topography, load and materials. *Trans. STLE*, Vol. 39, pp. 67-74.
- Lie, Y.; Bhat, R. B.** (1995): Coupled dynamics of a rotor-journal bearing system equipped with thrust bearings. *Shock and Vibration*, Vol. 2, No. 1, pp. 1-14.
- Nehari, Z.** (1975): Conformal mapping. Publisher: New York : Dover Publications.
- Patir, N.; Cheng, H. S.** (1978): An average flow model for determining effects of three-dimensional roughness on partial hydrodynamic lubrication. *Journal of Lubrication Technology*, Vol. 100, pp. 12-17.
- Pander, S. S.** (1986): Analysis of tapered land aerostatic

bearings for combined radial and thrust loads (Yates' Configuration). *Wear*, Vol. 107, pp. 299-315.

Pander, S. S.; Pandit, M. D. (1986): Analysis of orifice compensated aerostatic bearings for combined radial and thrust Loads (Yates' Configuration). 12th AIMTDR Conference, IIT, Delhi, pp. 28-32.

Tawfik, M.; Stout, K. J. (1981): Combined radial and thrust aerostatic bearings-a summary. Proc. 8th International Gas Bearing Symposium, April 8-10, 1981, BHRA Fluid Engineering, Cranfield, Beds., 1981, Paper 13.

Tieu, A. K. (1991): Hydrodynamic thrust bearings: theory and experiment. *Journal of Tribology*, Vol. 113, pp. 633-638.

Wang, Y.; Zhang, C.; Wang, Q.; Lin, C. (2002): A mixed-TEHD analysis and experiment of journal bearings under severe operating conditions," Accepted by *Tribology International*

Zang, Y.; Hatch, M. R. (1995): Analysis of coupled journal and thrust hydrodynamic bearing using a finite-volume method. *Advances in Information Storage and Processing Systems*, ASME Vol. 1, pp. 71-78.

Zhang, Q. D. (1999): Design of a hybrid fluid bearing system for HDD spindles. *IEEE transactions on magnetics*, Vol. 35, pp. 821-826.